

UC Davis

UC Davis Previously Published Works

Title

A Fibrosis-Independent Hepatic Transcriptomic Signature Identifies Drivers of Disease Progression in Primary Sclerosing Cholangitis

Permalink

<https://escholarship.org/uc/item/8357c68p>

Journal

Hepatology, 73(3)

ISSN

0270-9139

Authors

Gindin, Yevgeniy

Chung, Chuhan

Jiang, Zhaoshi

et al.

Publication Date

2021-03-01

DOI

10.1002/hep.31488


Copyright Information

This work is made available under the terms of a Creative Commons Attribution-NonCommercial-NoDerivatives License, available at

<https://creativecommons.org/licenses/by-nc-nd/4.0/>

Peer reviewed

A Fibrosis-Independent Hepatic Transcriptomic Signature Identifies Drivers of Disease Progression in Primary Sclerosing Cholangitis

Yevgeniy Gindin,¹ Chuhan Chung,¹ Zhaoshi Jiang,¹ Jing Zhu Zhou,¹ Jun Xu,¹ Andrew N. Billin,¹ Robert P. Myers,¹ Zachary Goodman,² Abdolamir Landi,³ Michael Houghton,³ Richard M. Green,⁴ Cynthia Levy,⁵ Kris V. Kowdley,⁶ Christopher L. Bowlus,⁷ Andrew J. Muir ,⁸ and Michael Trauner⁹

BACKGROUND AND AIMS: Primary sclerosing cholangitis (PSC) is a heterogeneous cholangiopathy characterized by progressive biliary fibrosis. RNA sequencing of liver tissue from patients with PSC ($n = 74$) enrolled in a 96-week clinical trial was performed to identify associations between biological pathways that were independent of fibrosis and clinical events.

APPROACH AND RESULTS: The effect of fibrosis was subtracted from gene expression using a computational approach. The fibrosis-adjusted gene expression patterns were associated with time to first PSC-related clinical event (e.g., cholangitis, hepatic decompensation), and differential expression based on risk groups and Ingenuity Pathway Analysis were performed. Baseline demographic data were representative of PSC: median age 48 years, 71% male, 49% with inflammatory bowel disease, and 44% with bridging fibrosis or cirrhosis. The first principle component (PC1) of RNA-sequencing data accounted for 18% of variance and correlated with fibrosis stage ($\rho = -0.80$; $P < 0.001$). After removing the effect of fibrosis-related genes, the first principle component was not associated with fibrosis ($\rho = -0.19$; $P = 0.11$), and a semisupervised clustering approach identified two distinct patient clusters with differential risk of time to first

PSC-related event ($P < 0.0001$). The two groups had similar fibrosis stage, hepatic collagen content, and α -smooth muscle actin expression by morphometry, Enhanced Liver Fibrosis score, and serum liver biochemistry, bile acids, and IL-8 (all $P > 0.05$). The top pathways identified by Ingenuity Pathway Analysis were eukaryotic translation inhibition factor 2 (eIF2) signaling and regulation of eIF4/p70S6K signaling. Genes involved in the unfolded protein response, activating transcription factor 6 (ATF6) and eIF2, were differentially expressed between the PSC clusters (down-regulated in the high-risk group by log-fold changes of -0.18 [$P = 0.02$] and -0.16 [$P = 0.02$], respectively). Clinical events were enriched in the high-risk versus low-risk group (38% [12/32] vs. 2.4% [1/42], $P < 0.0001$).

CONCLUSIONS: Removing the contribution of fibrosis-related pathways uncovered alterations in the unfolded protein response, which were associated with liver-related complications in PSC. (HEPATOLOGY 2021;73:1105-1116).

Primary sclerosing cholangitis (PSC) is a heterogeneous and progressive cholangiopathy characterized by chronic inflammation and

Abbreviations: ATF6, activating transcription factor 6; BA, bile acid; C4, 7 α -hydroxy-4-cholesten-3-one; CHOP, C/EBP homologous protein; eIF2, eukaryotic translation inhibition factor 2; ELF, Enhanced Liver Fibrosis; ER, endoplasmic reticulum; FGF19, fibroblast growth factor 19; FXR, farnesoid X receptor; IQR, interquartile range; PC, principal component; PSC, primary sclerosing cholangitis; RNA-seq, RNA sequencing; UDCA, ursodeoxycholic acid; UPR, unfolded protein response; XBP1, X-box binding protein 1; α -SMA, alpha-smooth muscle actin.

Received May 15, 2020; accepted July 7, 2020.

Additional Supporting Information may be found at onlinelibrary.wiley.com/doi/10.1002/hep.31488/supinfo.

This study was supported by Gilead Sciences.

© 2020 The Authors. HEPATOLOGY published by Wiley Periodicals LLC on behalf of American Association for the Study of Liver Diseases. This is an open access article under the terms of the Creative Commons Attribution-NonCommercial-NoDerivs License, which permits use and distribution in any medium, provided the original work is properly cited, the use is non-commercial and no modifications or adaptations are made.

View this article online at [wileyonlinelibrary.com](https://onlinelibrary.wiley.com).

DOI 10.1002/hep.31488

scarring of the intrahepatic and/or extrahepatic bile ducts. The pathogenesis of PSC remains incompletely understood, and currently no therapy outside of liver transplantation improves clinical outcomes.^(1,2) The regional variability of the histologic features of PSC limits the use of liver biopsy in routine clinical practice, although some studies demonstrate a prognostic role for histology-based scores.⁽³⁾ A recent controlled clinical trial demonstrated that the stage of fibrosis determined histologically or based on noninvasive markers (e.g., Enhanced Liver Fibrosis score [ELF], liver stiffness by transient elastography) is predictive of liver-related complications in patients with PSC.⁽⁴⁾ Indeed, the primary endpoint of two ongoing phase 3 trials of therapies for PSC includes nonprogression of liver fibrosis determined histologically (NCT03872921; NCT03890120).

The etiology of PSC likely reflects interactions between known genetic risk loci and environmental factors.^(5,6) The shared genetic risk loci with other autoimmune diseases emphasizes genetic susceptibility and immune dysfunction. These genetic associations, however, do not explain the widely varying disease manifestations that occur with other autoimmune diseases or within PSC itself, given the rarity of developing PSC in patients with similar risk loci.

The absence of clinical benefit in trials using a host of immunosuppressive therapies speaks to the limitation of suppressing inflammation alone in PSC.⁽⁷⁾ Thus, patient-specific environmental risk factors and highly variant genetics combine to generate a widely variable clinical phenotype.

Given the elusive nature of PSC pathogenesis, we undertook RNA sequencing (RNA-seq), an unbiased approach to analysis of the hepatic transcriptome, using liver biopsies obtained from patients with PSC enrolled in a randomized controlled trial.⁽⁴⁾ Patients with PSC across the spectrum of fibrosis severity were enrolled, and a bioinformatics approach was used to identify drivers of PSC pathogenesis. We hypothesized that removing the influence of fibrosis-related genes could potentially reveal biologic determinants of PSC pathogenesis.

Materials and Methods

STUDY POPULATION AND OUTCOMES

The PSC study population was derived from a phase 2b, placebo-controlled trial of simtuzumab, a

Potential conflict of interest: Jing Zhu Zhou is a contractor for Gilead Sciences. Dr. Gindin is employed and owns stock in Gilead. Dr. Chung is employed and owns stock in Gilead. Dr. Jiang is employed and owns stock in Gilead. Dr. Xu is employed and owns stock in Gilead. Dr. Billin is employed and owns stock in Gilead. Dr. Myers is employed and owns stock in Gilead. Dr. Levy received grants from Intercept, Gilead, Genfit, Mirum, HighTide, and Durect. Dr. Kowdley consults, advises, and received grants from Conatus. He advises, is on the speakers' bureau, and received grants from Intercept and Gilead. He consults and received grants from CymaBay. He advises and received grants from HighTide and Genfit. He consults for Assembly, Blade, and Roche. He advises Boehringer-Ingelheim, is on the speakers' bureau for AbbVie, and received grants from Allergan, Novartis, and Enanta. Dr. Borwul consults and received grants from Gilead, Intercept, CymaBay, BiomX, and GlaxoSmithKline. He received grants from Takeda and Novartis. Dr. Trauner consults, is on the speakers' bureau, and received grants from Falk, Gilead, Intercept, and MSD. He consults and received grants from Albireo. He is on the speakers' bureau and received travel grants from Roche. He consults for BiomX, Boehringer Ingelheim, Genfit, Novartis, Phenex, and Regulus. He received grants from CymaBay, Takeda, and travel grants from AbbVie.

ARTICLE INFORMATION:

From the ¹Gilead Sciences, Inc., Foster City, CA; ²Inova Fairfax Hospital, Falls Church, VA; ³Department of Medical Microbiology and Immunology, Li Ka Shing Institute of Virology, University of Alberta, Edmonton, AB, Canada; ⁴Division of Gastroenterology and Hepatology, Department of Medicine, Feinberg School of Medicine at Northwestern University, Chicago, IL; ⁵University of Miami, Miami, FL; ⁶Liver Institute Northwest, Seattle, WA; ⁷Division of Gastroenterology and Hepatology, University of California at Davis, Sacramento, CA; ⁸Duke University School of Medicine, Durham, NC; ⁹Division of Gastroenterology and Hepatology, Department of Medicine III, Medical University of Vienna, Vienna, Austria.

ADDRESS CORRESPONDENCE AND REPRINT REQUESTS TO:

Michael Trauner, M.D.
Division of Gastroenterology and Hepatology
Internal Medicine III, Medical University of Vienna
Währinger Gürtel 18-20

A-1090 Vienna, Austria
E-mail: michael.trauner@meduniwien.ac.at
Tel.: 43(0)1/40400-47410

monoclonal antibody directed against lysyl oxidase-like 2 (NCT01672853). The design and results of this trial have been described.⁽⁴⁾ In brief, adult patients with compensated, large-duct PSC were randomized to receive weekly subcutaneous injections of simtuzumab (either 75 mg or 125 mg) or placebo for 96 weeks. Percutaneous liver biopsies were obtained in a protocol-specified manner with a central pathologist (Z.G.) interpreting the adequacy of the biopsy specimen for diagnosis and staging of PSC.⁽⁴⁾ The primary objective of the study was to evaluate whether simtuzumab was effective in preventing histologic progression of fibrosis, as measured by changes in hepatic collagen content. The study was approved by the institutional review boards of participating institutions, and all patients provided written informed consent, including for genomic sequencing, before participation in the study.

The hepatic transcriptomic analysis was restricted to baseline liver biopsy samples (see subsequently). Biopsies were reviewed by a central pathologist who staged fibrosis according to the Ishak classification. Patients were categorized as having no to mild fibrosis (Ishak stages 0-1), moderate fibrosis (stages 2-4), or cirrhosis (stages 5-6). Morphometric quantification of hepatic collagen content and alpha-smooth muscle actin (α -SMA) expression were also performed, as previously described.⁽⁴⁾ The outcome of interest for the study was time to first PSC-related clinical event, defined as ascending cholangitis, sepsis, hepatic decompensation (i.e., ascites, variceal hemorrhage, hepatic encephalopathy), cholangiocarcinoma, hepatocellular carcinoma, liver transplantation, or death during the 96-week duration of the study. In patients with multiple clinical events, the earliest onset event was reported.

HEPATIC TRANSCRIPTOMIC ANALYSIS

RNA-seq (SureSelect protocol) was analyzed on formalin-fixed, paraffin-embedded liver biopsies ($n = 74$). RNA quality control was assessed by DV200 > 10%, with an initial collection from $n = 84$, with $n = 6$ failing to meet the DV200 threshold and another 4 patients lost to clinical follow-up. Gene expression was quantified using Salmon.⁽⁸⁾ A semisupervised bioinformatics approach was used to identify in-tissue, fibrosis-independent gene expression

signatures associated with time to first PSC-related clinical event. Specifically, the effect of fibrosis was subtracted from gene expression (as implemented in the “removeBatchEffect” function in R package limma)⁽⁹⁾ by first fitting a linear model to each gene, relating its expression to fibrosis stage, and then subtracting the portion of gene expression that can be accounted for by fibrosis. This method had the net effect of removing genes with expression that is highly correlated with fibrosis stage. A Cox proportional hazards regression model was fit onto every gene after fibrosis correction to select genes with a significant association with PSC-related clinical events (unadjusted P value ≤ 0.05). Patient clustering, using genes associated with clinical events as input after adjusting for fibrosis, was carried out using a consensus clustering algorithm.^(10,11) Consensus clustering ascertains the confidence in the number of clusters (here patient clusters) present in the data, as well as the robustness of these clusters to random sampling. Differential expression based on the identified clusters was performed using limma-voom.⁽¹²⁾ P values were corrected for multiple testing where appropriate.

INGENUITY PATHWAY ANALYSIS

RNA-seq data were analyzed using Ingenuity Pathway Analysis software (Ingenuity Systems, Redwood City, CA) to examine for transcriptional networks associated with biological signaling. Scores were used to rank signaling and pathway networks according to their function.

BIOMARKERS OF BILE ACID HOMEOSTASIS, LIVER FIBROSIS, AND IL-8

Levels of total bile acids (BAs) and 15 specific BA species were quantified by liquid chromatography-tandem mass spectrometry (LC/MS-MS; Agilent 1290/Sciex; Metabolon, Durham, NC) in fasting serum samples obtained at baseline ($n = 40$). In addition, we measured the serum levels of 7 α -hydroxy-4-cholesten-3-one (C4), a precursor in BA synthesis, by LC/MS-MS, and serum levels of fibroblast growth factor 19 (FGF19), a hormone that serves as the inhibitory signal for CYP7A1, the rate-limiting enzyme in BA synthesis, by Quantikine enzyme-linked immunosorbent assay (R&D, Minneapolis, MN). ELF score

(Siemens Healthcare, Erlangen, Germany), a noninvasive marker of liver fibrosis, was tested according to manufacturer's specifications. IL-8 protein was measured by a commercial multiplex assay (Meso Scale Diagnostics, Rockville, MD).

STATISTICAL ANALYSES

Comparisons between groups were made using Wilcoxon rank sum tests, and correlations between parameters using Spearman correlations. Time to first PSC-related clinical event was assessed using Kaplan-Meier analysis and Cox proportional hazards regression using the survival R package version 2.41.⁽¹³⁾

Results

STUDY POPULATION

In total, 74 patients with compensated, large-duct PSC were included in the current study. Their demographics and baseline characteristics are given in Table 1. The mean age was 46 years, 70% were male, 81% were Caucasian, 50% had ulcerative colitis, and 68% were prescribed ursodeoxycholic acid (UDCA). Eleven patients (15%) had cirrhosis (Ishak stages 5-6) on baseline liver biopsy.

PRINCIPAL COMPONENT ANALYSIS IDENTIFIES FIBROSIS-RELATED GENES AS PRIMARY DRIVERS OF GENE-EXPRESSION DIFFERENCES ACROSS FIBROSIS STAGES

The first principal component (PC1) of the RNA-seq data accounted for 18% of variance in hepatic gene expression (Fig. 1A and Supporting Fig. S1). Without adjustment for fibrosis stage, PC1 derived from the gene-expression data was highly correlated with Ishak fibrosis stage at the individual patient level (Spearman $\rho = -0.80$; $P < 0.001$) (Fig. 1B). As expected, the most highly up-regulated pathways according to pathway analysis were those involved in fibrogenesis, specifically genes involved in cell adhesion and cell-matrix interactions ($P = 1.60 \times 10^{-21}$) and stellate cell activation and liver fibrosis ($P = 1.28 \times 10^{-12}$) (Supporting Table S1).

TABLE 1. Baseline Demographics and Clinical Characteristics of the Study Population

Characteristic	Total (n = 74)
Demographics	
Age, years	46.3 (11.3)
Female	22 (30)
Body mass index, kg/m ²	26.9 (4.8)
UDCA use	50 (68)
Ulcerative colitis	37 (50)
Ethnicity	
European descent	60 (81)
African-American	12 (16)
Asian	2 (3)
Liver tests	
Alanine aminotransferase, U/L	85.1 (72.7)
Alkaline phosphatase, U/L	332.6 (302.4)
Gamma-glutamyltransferase, U/L	408.6 (457.4)
Bilirubin, mg/dL	1.1 (1.3)
Albumin, g/dL	4.0 (0.4)
International normalized ratio	1.0 (0.2)
Platelets, $\times 10^3/\mu\text{L}$	260.5 (98.0)
Other biomarkers	
ELF	9.47 (1.35)
Hyaluronic acid, ng/mL	100.8 (188.2)
TIMP-1, ng/mL	331.3 (163.7)
PIII-NP, ng/mL	9.6 (5.7)
Hemoglobin, g/dL	13.9 (1.7)
Total bile acids, pg/mL	1590.2 (586.2, 3649.2)*
C4, ng/mL	8.6 (4.3, 24.6)
FGF19, pg/mL	135.8 (60.4, 221.4)
IL-8, pg/mL	19.5 (12.0, 41.0)
Liver histology	
Ishak fibrosis stage	
F0-F1	26 (35)
F2-F4	37 (50)
F5-F6	11 (15)
Hepatic collagen content, %	5.3 (5.1)
α -SMA expression, %	5.3 (7.7)

Note: All data are presented as mean (SD) or n (%). Serum bile acids, C4, and FGF19 data are available for n = 40 subjects.

*UDCA and UDCA conjugates were removed from the BA pool. Abbreviations: PIII-NP, type III procollagen peptide; TIMP-1, tissue inhibitor of metalloproteinase 1.

REMOVING THE EFFECT OF FIBROSIS IDENTIFIES TWO PATIENT SUBGROUPS WITH DISTINCT RISK OF PSC-RELATED CLINICAL EVENTS

A bioinformatics approach was used to determine whether patients could be stratified according to the

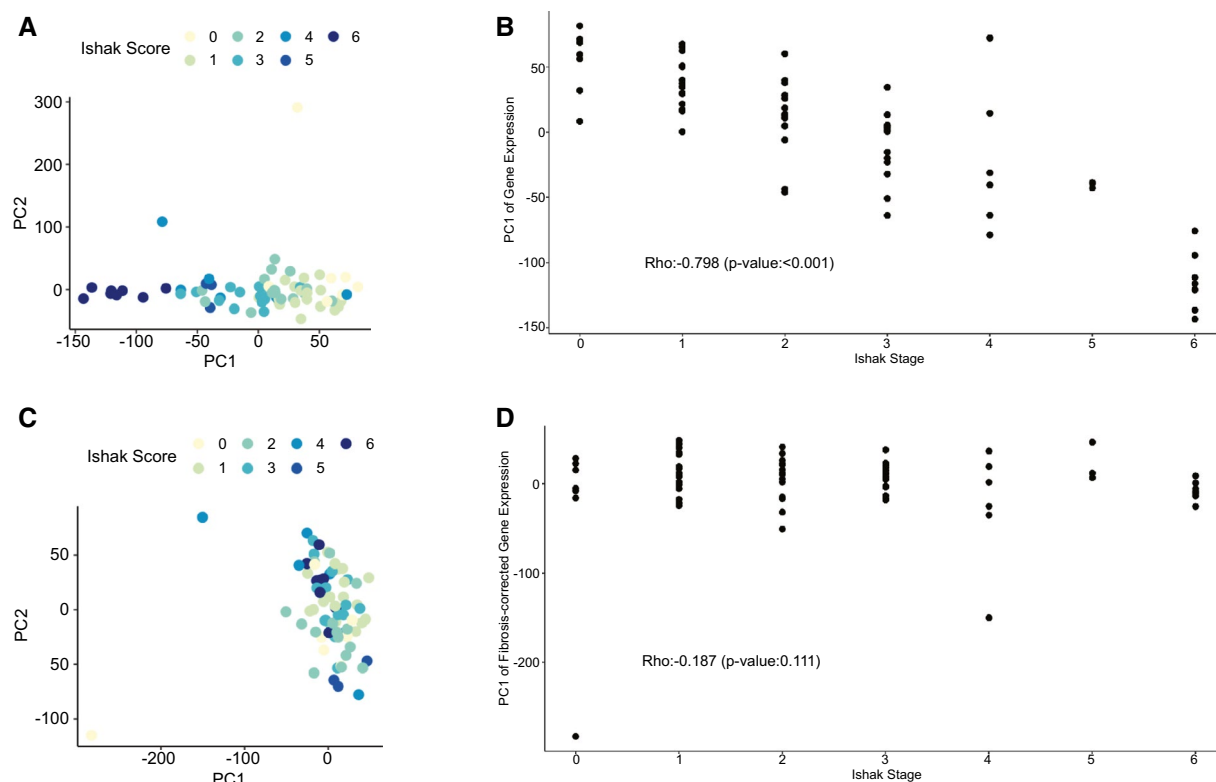


FIG. 1. Principal components in gene-expression data. Each dot represents a patient; color represents Ishak fibrosis stages. (A) Principal components (PC1 and PC2) without removing the effects of fibrosis from gene expression. (B) PC1 mapped according to Ishak fibrosis stage. (C) Principal components after removing the effects of fibrosis from gene expression. (D) PC1 mapped according to Ishak fibrosis stage after subtracting fibrosis-related genes from gene expression.

risk of PSC-related clinical events based on biologic pathways devoid of the influence of fibrosis-related genes and pathways. After removing the effect of fibrosis on gene-expression data, PC1 was no longer associated with the stage of fibrosis ($\rho = -0.19$; $P = 0.11$; Fig. 1C,D). This approach yielded two distinct clusters of patients with PSC according to the risk of PSC-related clinical events, herein referred to as “low-risk” ($n = 42$) and “high-risk” ($n = 32$) groups (Fig. 2A). As shown in Fig. 2B, survival free of clinical events was significantly greater in the low-risk versus high-risk group (log-rank $P < 0.001$). During a median follow-up of 23 months (interquartile range [IQR], 22.52, 23.25), 1 of 42 patients (2.4%) in the low-risk group experienced clinical events ($n = 1$, ascending cholangitis), while 12 of 32 patients (38%) in the high-risk group had events (ascending cholangitis [$n = 7$], cholangiocarcinoma [$n = 2$], hepatic

encephalopathy [$n = 1$], jaundice [$n = 1$]), and sepsis [$n = 1$]).

To confirm the ability of the bioinformatics approach to remove the influence of fibrosis-related gene-expression pathways on the patient clustering, the clinical characteristics of the two clusters were compared. As indicated in Table 2, no differences in demographic parameters, UDCA use, liver biochemistry, platelets, ELF score, or hepatic collagen content or α -SMA expression by morphometry were observed between the low-risk and high-risk clusters. Importantly, the distribution of fibrosis stages was nearly identical between groups: 14% of the low-risk group and 16% of the high-risk group had cirrhosis at baseline ($P = 1.00$). Thus, a fibrosis-independent, hepatic gene-expression signature stratifies patients with PSC into two discrete clusters with distinct prognoses.

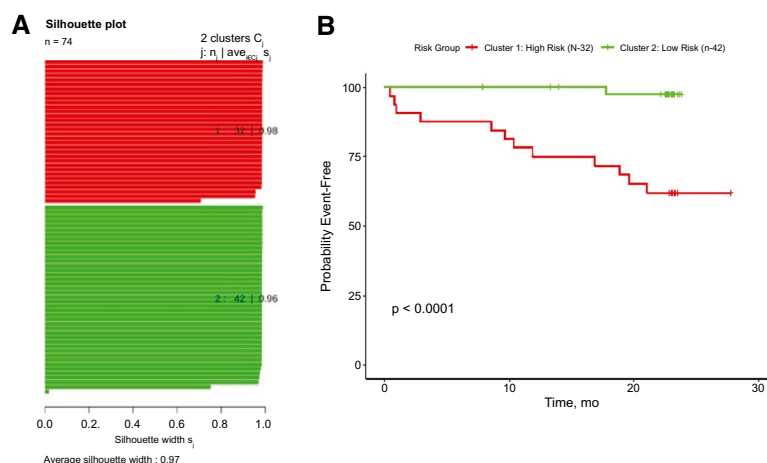


FIG. 2. Liver fibrosis-adjusted PSC clusters. (A) Gene expression clustering of fibrosis-corrected data. Each bar represents a gene-expression profile of a patient with PSC; color represents cluster assignment; and bar length represents the confidence of cluster assignment. (B) Kaplan-Meier curve comparing survival free of PSC-related clinical events of patients in two clusters defined by fibrosis-adjusted hepatic gene-expression signature.

GENES INVOLVED IN THE ADAPTIVE RESPONSE TO ENDOPLASMIC RETICULUM STRESS ARE DIFFERENTIALLY EXPRESSED AFTER FIBROSIS EXCLUSION BUT NOT ASSOCIATED WITH MARKERS OF BA HOMEOSTASIS

Pathway analysis revealed that multiple components of the unfolded protein response (UPR) were significantly down-regulated in the high-risk patient cluster (highlighted in red in Fig. 3). Among these genes were activating transcription factor 6 (*ATF6*), a transcriptional regulator of endoplasmic reticulum (ER) chaperones that facilitate protein folding, and eukaryotic translation inhibition factor 2 α (*eIF2 α*), an enzyme necessary for protein translation. Expression of these genes was down-regulated in the high-risk group compared with the low-risk group by log-fold changes of -0.18 ($P = 0.02$) and -0.16 ($P = 0.02$), respectively. The list of the top differentially expressed genes in the high-risk versus low-risk groups revealed other components of the protein translational apparatus and structural adhesion proteins (Table 3).

Experimental models of PSC postulate a role for BAs in the induction of the UPR, an effect that may be mediated in part by activation of the farnesoid X receptor (FXR).⁽¹⁴⁾ However, serum levels of multiple

BAs, including those that serve as the endogenous ligands for FXR, were similar in the low-risk and high-risk patient clusters (Table 4 and Supporting Table S2). Subtracting the contribution of UDCA resulted in similar levels of BAs between clusters. Pooled assessments of the endogenous FXR agonists (chenodeoxycholic acid, deoxycholic acid, and cholic acid) alone and combined also demonstrated similar levels between the two groups (Supporting Table S2). Moreover, serum levels of C4 and FGF19 were similar, suggesting similarities in FXR signaling between the two clusters. In contrast, differential expression of genes involved in the uptake and excretion of BAs was seen. The gene for OATP-C (*SLCO1B1*) was significantly reduced ($P < 0.001$) in the high-risk cluster, and a trend toward significance in the gene for bile salt export pump was also apparent ($P = 0.15$) (Supporting Fig. S2). Expression of other genes involved in BA uptake, including NTCP (*SLC10A1*), did not show significant differences. Thus, differences in UPR expression seen in the two patient clusters were not clearly related to BA levels, although differential expression of some transporters was apparent.

Levels of the key neutrophil chemoattractant IL-8 in serum and bile have been associated with worse clinical outcomes in patients with PSC and can be elicited by the UPR.⁽¹⁵⁻¹⁷⁾ As such, we compared the hepatic expression and serum levels of IL-8 between the two PSC patient clusters. As shown in Fig. 4, median serum levels of IL-8

TABLE 2. Baseline Demographics and Clinical Characteristics of Patients With PSC According to Gene-Expression Signature Cluster

Characteristic	Low-Risk Subgroup (n = 42)	High-Risk Subgroup (n = 32)	P Value
Demographics			
Age, years	45.1 (11.5)	47.7 (11.0)	0.23
Female	13 (31)	9 (28)	0.99
Body mass index, kg/m ²	26.1 (4.6)	27.9 (5.1)	0.10
UDCA use	28 (67)	22 (69)	1.00
Ulcerative colitis	18 (43)	19 (59)	0.24
Ethnicity			
European descent	32 (76)	28 (88)	0.46
African-American	8 (19)	4 (12)	
Asian	2 (5)	0	
Liver tests			
Alanine aminotransferase, U/L	91.1 (83.3)	77.2 (56.3)	0.97
Alkaline phosphatase, U/L	317.0 (305.3)	352.9 (302.2)	0.48
Gamma-glutamyltransferase, U/L	413.3 (487.6)	402.3 (422.1)	0.74
Bilirubin, mg/dL	1.2 (1.2)	1.1 (1.4)	0.62
Albumin, g/dL	4.0 (0.4)	4.0 (0.5)	0.91
International normalized ratio	1.0 (0.2)	1 (0.1)	0.98
Platelets, $\times 10^3/\mu\text{L}$	267.9 (104.0)	250.9 (90.0)	0.46
Other biomarkers			
ELF	9.3 (1.5)	9.7 (1.2)	0.25
Hyaluronic acid, ng/mL	104.1 (225.8)	96.5 (126.1)	0.07
TIMP-1, ng/mL	320.1 (161.1)	346.0 (168.4)	0.41
PIII-NP, ng/mL	9.4 (5.6)	9.9 (5.8)	0.71
Hemoglobin, g/dL	13.8 (1.6)	14.0 (1.9)	0.68
Liver histology			
Ishak fibrosis stage			
F0-F1	15 (36)	11 (34)	1.00
F2-F4	21 (5)	16 (5)	
F5-F6	6 (14)	5 (16)	
Hepatic collagen content, %	5.2 (4.3)	5.5 (6.1)	0.81
α -SMA expression, %	5.4 (8.0)	5.0 (7.5)	0.87

Note: All data are presented as mean (SD) or n (%).

Abbreviations: PIII-NP, type III procollagen peptide; TIMP-1, tissue inhibitor of metalloproteinase 1.

were similar between the low-risk and high-risk clusters (17.5 vs. 21.5 pg/mL; $P = 0.62$), whereas the hepatic expression of the IL-8 gene, CXCL8, was higher in patients at increased risk for clinical events ($P = 0.076$). Whether the decreased expression of genes that comprise an adaptive ER stress response are associated with potentially higher cytokine responses is unknown.

Discussion

In the current study, we hypothesized that a bioinformatics approach that removed the influence of

fibrosis-related genes in the hepatic transcriptome could potentially identify determinants of PSC pathogenesis. An initial effort to remove the influence of fibrosis-related genes identified a prognostic signature of nine genes related to immune responses and cell adhesion proteins, but incompletely removed the influence of fibrosis.⁽¹⁸⁾ However, the current approach eliminated the influence of fibrosis, as evidenced by similar histologic (e.g., Ishak stage, hepatic collagen content, α -SMA expression) and nonhistologic (e.g., ELF score, liver biochemistry, platelets) parameters of fibrosis between two patient groups characterized by distinct gene-expression profiles

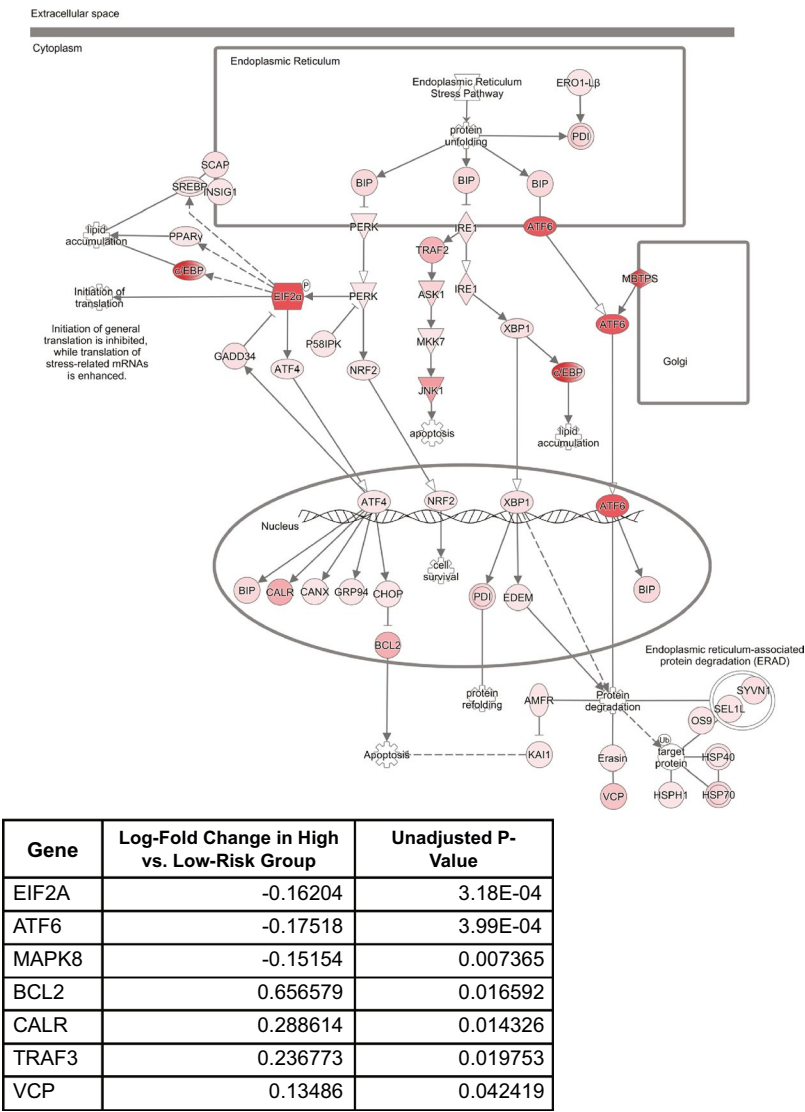


FIG. 3. UPR pathway highlighting gene-expression differences between the low-risk and high-risk PSC clusters. The nodes in the pathway are shaded proportional to the *P* value of differential gene expression between low-risk and high-risk PSC clusters. Genes with smaller *P* values are darker. Differentially expressed genes associated with this pathway are provided in the table as an inset. The pathway diagram was generated using Ingenuity Pathway Analysis. Abbreviations: ASK1, mitogen-activated protein kinase kinase 5; ATF4, activating transcription factor 4; ATF6, activating transcription factor 6; BCL2, BCL2 apoptosis regulator; BIP, heat shock protein family A (Hsp70) member 5; c/EBP, CCAAT Enhancer Binding Protein Beta; CALR, calreticulin; CANX, calnexin; CHOP, DNA damage inducible transcript 3; EDEM, ER degradation enhancing alpha-mannosidase like protein 1; EIF2 α , eukaryotic translation initiation factor 2A; ERO1-L β , endoplasmic reticulum oxidoreductase 1 beta; GADD34, protein phosphatase 1 regulatory subunit 15A; GRP94, heat shock protein 90 beta family member 1; INSIG1, insulin induced gene 1; IRE1, endoplasmic reticulum to nucleus signaling 1; JNK1, mitogen-activated protein kinase 8; MBTPS, membrane bound transcription factor peptidase; MKK7, mitogen-activated protein kinase kinase 7; NRF2, “nuclear factor, erythroid 2 like 2”; P58IPK, DnaJ heat shock protein family (Hsp40) member C3; PDI, protein disulfide isomerase; PERK, eukaryotic translation initiation factor 2 alpha kinase 3; PPAR γ , peroxisome proliferator activated receptor gamma; SCAP, SREBF chaperone; SREBF, sterol regulatory element binding transcription factor; TRAF2, TNF receptor associated factor 2; XBP1, X-box binding protein 1.

and prognoses. The incidence of PSC-related clinical events was markedly different between the two clusters, with a greater number of events, including events of hepatic decompensation, in the high-risk subgroup compared with a single case of ascending cholangitis in the low-risk group. Interrogation of

TABLE 3. Top Differentially Expressed Genes in Patients With High Risk of Clinical Events

Gene*	Log-Fold Change in High Vs. Low-Risk Group	Unadjusted PValue	Adjusted PValue
EIF3E	-0.30195	6.08E-09	0.000112
ARHGAP5	-0.22756	2.44E-08	0.000184
AGRN	0.495281	3.00E-08	0.000184
CEBPZOS	-0.43928	1.14E-07	0.000487
CEP170B	0.310916	1.47E-07	0.000487
SBNO2	0.356272	1.59E-07	0.000487
EIF4A2	-0.20602	2.83E-07	0.000666
NOTCH1	0.296809	2.90E-07	0.000666
GRK2	0.25534	4.96E-07	0.001013
HCFC1	0.236412	5.81E-07	0.001068
CEBPZ	-0.19753	7.88E-07	0.001315
PIEZO1	0.371143	9.00E-07	0.001378
MCRS1	0.298438	1.07E-06	0.001512
ACAP3	0.31977	1.29E-06	0.001621
GOLGA3	0.298354	1.41E-06	0.001621
TECPR1	0.307899	1.49E-06	0.001621
FANCL	-0.27802	1.50E-06	0.001621
AUH	-0.31464	1.60E-06	0.001631
FLII	0.270343	1.70E-06	0.001639
MICALL1	0.338758	1.95E-06	0.001704

Abbreviations: ACAP3, ArfGAP with coiled-coil, ankyrin repeat and PH domains 3; AGRN, agrin; ARHGAP5, Rho GTPase activating protein 5; AUH, AU RNA binding methylglutaconyl-CoA hydratase; CEBPZ, CCAAT enhancer binding protein zeta; CEBPZOS, CEBPZ opposite strand; CEP170B, centrosomal protein 170B; EIF3E, eukaryotic translation initiation factor 3 subunit E; EIF4A2, eukaryotic translation initiation factor 4A2; FANCL, FA complementation group L; FLII, FLII actin remodeling protein; GOLGA3, golgin A3; GRK2, G protein-coupled receptor kinase 2; HCFC1, host cell factor C1; MCRS1, microspherule protein 1; MICALL1, MICAL like 1; NOTCH1, notch receptor 1; PIEZO1, piezo type mechanosensitive ion channel component 1; SBNO2, strawberry notch homolog 2; TECPR1, tectonin beta-propeller repeat containing 1.

*Genes are sorted according to increasing order of *P* values.

the gene signatures from these two groups revealed differential expression of key components of the UPR, including *ATF6* and *eIF2* (specifically, reduced expression of these genes in patients with a high incidence of complications). These findings suggest that the UPR may be a critical biologic determinant of clinical outcomes in PSC.

The UPR is a central cellular homeostatic pathway that becomes active when the protein folding capacity of the endoplasmic reticulum is exceeded. The resultant “ER stress” results in the toxic accumulation of unfolded or misfolded proteins.⁽¹⁹⁾ Three transmembrane protein sensors are involved in this homeostatic

mechanism to detect unfolded proteins in the ER: PKR-like ER kinase (PERK), inositol-requiring enzyme 1 α (IRE1 α), and ATF6.^(20,21) Activation of PERK leads to inactivation of eIF2 α , which blocks protein synthesis. ATF6 translocation from the ER to the Golgi apparatus and its subsequent proteolytic cleavage leads to nuclear translocation and transcriptional regulation of other genes that coordinate the UPR, including C/EBP homologous protein (*CHOP*) and X-box binding protein 1 (*XBPI*).

Previous experimental work has demonstrated associations between cholestasis and an abnormal UPR.^(14,21-23) However, whether the UPR serves to protect or worsen cellular injury in PSC remains unclear from these studies. Knockdown of *CHOP* reduces liver injury in the acute setting of bile duct ligation, thereby suggesting a harmful role for the UPR in this setting. Bile duct ligation, however, represents a poor model of chronic cholestasis in humans. In contrast, a beneficial role for the UPR is suggested by its induction in response to chronic feeding of toxic BAs such as lithocholic acid, which increases hepatic expression of both *Chop* and *Xbp1*.⁽²²⁾ Conversely, UDCA has been shown to attenuate the UPR in obese mice.⁽²⁴⁾ In the setting of elevated BAs found in PSC, mechanisms to reduce BA synthesis would appear to be protective. Despite these findings, we found no differences in total BAs, BA species, markers of BA homeostasis (i.e., C4, FGF19), or UDCA use between the two patient subgroups. In contrast, IL-8, a prognostic cytokine in PSC, demonstrated higher expression levels in hepatic tissue of high-risk patients in whom decreased components of the UPR were observed, a finding discordant with prior observations.⁽²⁵⁾ Of course, the current analysis was limited by the performance of measurements at a single time point and gene expression profiling only at baseline. Further investigation of these relationships with cholestasis in PSC will require longitudinal assessment of UPR-related gene expression and changes in BAs and cytokines.

Another recent study by our group demonstrating the impact of age acceleration in PSC may have relevance to the present findings.⁽²⁶⁾ In that study, a global epigenetic clock associated with an intrinsic rate of aging, the “Horvath clock,” demonstrated marked age acceleration in patients with PSC, far exceeding that found in other chronic liver diseases such as nonalcoholic steatohepatitis or hepatitis B, despite

TABLE 4. Markers of BA Homeostasis According to Subgroup of Patients With PSC

Parameter	Low-Risk Subgroup (n = 24)	High-Risk Subgroup (n = 16)	PValue
BA, pg/mL			
Total BA*	2,470.8 (656.47, 7,245.2)	2,017 (794.98, 7,500.33)	0.70
Total primary BA	1,635.1 (633.16, 6,235.3)	1,713.7 (581.15, 6,726.35)	0.81
Total secondary BA*	194.1 (34.79, 724.8)	202.8 (22.4, 457.4)	0.35
Total conjugated BA*	2,163.2 (642.8, 7,064.8)	1,871.4 (604.3, 7,368.9)	0.66
Total unconjugated BA*	116.0 (32, 237.0)	101.8 (31.8, 196.9)	0.51
CDCA	20.6 (5.8, 58.2)	19.3 (10.4, 66.6)	0.91
TCDCA	223 (33.3, 838)	182 (42.7, 765.5)	0.77
GCDCA	719 (185, 1540)	610 (198, 1,795)	0.81
CA	15 (3, 31.8)	12.2 (6.0, 18.3)	1.00
TCA	110 (13.3, 850)	152.5 (18.3, 1,424)	0.99
GCA	511 (80.2, 2,220)	449.5 (113.6, 2,410)	1.00
LCA	2.7 (2.5 [†] , 18.2)	2.5 [†] (2.5 [†] , 14)	0.62
TLCA	5 [†] (5 [†] , 8.3)	5 [†] (5 [†] , 9.31)	0.71
GLCA	11 (2.5 [†] , 67)	9.2 (2.5 [†] , 21.9)	0.53
DCA	53.3 (5 [†] , 136)	45.7 (5 [†] , 97.4)	0.76
TDCA	38.3 (5 [†] , 76)	12.7 (5 [†] , 57.4)	0.53
GDCA	78.2 (5.5, 307)	92.1 (2.5 [†] , 156.5)	0.55
C4, ng/mL	6.7 (4.1, 24.7)	12.8 (4.6, 37.4)	0.36
FGF19, pg/mL	147.3 (59.7, 222.2)	93.3 (60.7, 191.7)	0.58

Note: Data are presented as median (IQR).

*UDCA and UDCA conjugates removed from the BA pools.

[†]Bile acid levels below the lower limit of quantification (LLOQ) of the Metabolon assay were assigned to the value corresponding to LLOQ.

Abbreviations: CA, cholic acid; CDCA, chenodeoxycholic acid; DCA, deoxycholic acid; GCA, glycocholic acid; GCDCA, glycochenodeoxycholic acid; GDCA, glycodeoxycholic acid; GLCA, glycolithocholic acid; LCA, lithocholic acid; TCA, taurocholic acid; TCDCA, taurochenodeoxycholic acid; TDCA, taurodeoxycholic acid; TLCA, tauroolithocholic acid.

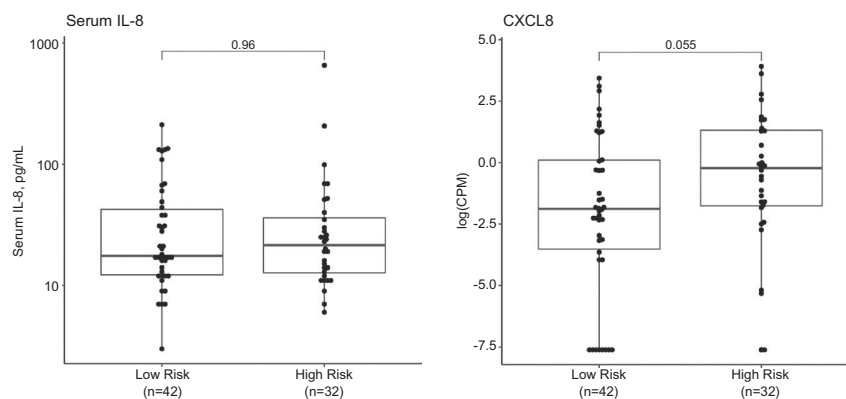


FIG. 4. Hepatic expression and serum levels of IL-8 according to the subgroup of patients with PSC. Hepatic IL-8 expression was normalized by median log2 expression levels of IL-8 in the low-risk population. The boxplots were presented as median (IQR).

the presence of advanced fibrosis in all groups.⁽²⁷⁻²⁹⁾ Related to these findings, multiple components of the UPR have been shown to decrease with advancing age and may contribute to multiple aging-related

diseases.⁽³⁰⁾ Whether the age acceleration identified in PSC contributes to the functional declines in the UPR with aging remains unknown. Determining this relationship will require future investigation of

clinical therapeutics that improve outcomes in PSC and evaluating the effects on UPR responses and age acceleration.

The bioinformatics analysis approach in the present study led to several clinical insights including the primacy of fibrogenic pathways in PSC and the suppression of key constituents of the UPR, the homeostatic response to ER stress, in those patients at higher risk of PSC-related complications. Given the chronicity of PSC and the patient-specific genetic and immune-mediated factors that influence the PSC phenotype, we hypothesized that removing the influence of fibrosis would uncover potential mediators in the pathogenesis of PSC. In fact, the UPR has been postulated to be involved in the pathogenesis of injury in multiple preclinical models of cholestasis.^(22,23) Several limitations of the study including the single time-point analysis of gene expression, small sample size and number of clinical events, and the need for further validation in translational studies do not obviate, we believe, the central finding that the UPR is dysregulated in clinical PSC.

In conclusion, the current bioinformatics analysis of hepatic transcriptomic data from liver biopsies of patients with PSC removed the influence of fibrosis-related genes and identified two distinct patient subgroups with marked imbalance in clinical complications. Differentially expressed components of the UPR, including *ATF6* in the high-risk patient subgroup, highlight potential deficiencies in the response to ER stress in those patients with PSC with a poor prognosis. These findings illustrate the potential of hepatic transcriptomic data to identify biologic drivers of PSC pathogenesis.

Author Contributions: Y.G., Z.J., C.C., and R.P.M. were responsible for the study design and data analysis. Y.G., C.C., R.P.M., and M.T. were responsible for drafting the manuscript. All authors reviewed the data and approved the final manuscript.

REFERENCES

- 1) Lazaridis KN, LaRusso NF. Primary sclerosing cholangitis. *N Engl J Med* 2016;375:2501-2502.
- 2) Karlsen TH, Folseraas T, Thorburn D, Vesterhus M. Primary sclerosing cholangitis—a comprehensive review. *J Hepatol* 2017;67:1298-1323.
- 3) de Vries EM, de Krijger M, Farkkila M, Arola J, Schirmacher P, Gotthardt D, et al. Validation of the prognostic value of histologic scoring systems in primary sclerosing cholangitis: an international cohort study. *HEPATOLOGY* 2017;65:907-919.
- 4) Muir AJ, Levy C, Janssen HLA, Montano-Loza AJ, Shiffman ML, Caldwell S, et al. Simtuzumab for primary sclerosing cholangitis: phase 2 study results with insights on the natural history of the disease. *HEPATOLOGY* 2019;69:684-698.
- 5) Karlsen TH, Boberg KM. Update on primary sclerosing cholangitis. *J Hepatol* 2013;59:571-582.
- 6) Karlsen TH. A lecture on the genetics of primary sclerosing cholangitis. *Dig Dis* 2012;30(Suppl. 1):32-38.
- 7) Lynch KD, Chapman RW, Keshav S, Montano-Loza AJ, Mason AL, Kremer AE, et al. Effects of vedolizumab in patients with primary sclerosing cholangitis and inflammatory bowel diseases. *Clin Gastroenterol Hepatol* 2020;18:179-187.e176.
- 8) Patro R, Duggal G, Love MI, Irizarry RA, Kingsford C. Salmon provides fast and bias-aware quantification of transcript expression. *Nat Methods* 2017;14:417-419.
- 9) Ritchie ME, Phipson B, Wu D, Hu Y, Law CW, Shi W, et al. limma powers differential expression analyses for RNA-sequencing and microarray studies. *Nucleic Acids Res* 2015;43:e47.
- 10) Xu T, Le TD, Liu L, Su N, Wang R, Sun B, et al. CancerSubtypes: an R/Bioconductor package for molecular cancer subtype identification, validation and visualization. *Bioinformatics* 2017;33:3131-3133.
- 11) Wilkerson MD, Hayes DN. ConsensusClusterPlus: a class discovery tool with confidence assessments and item tracking. *Bioinformatics* 2010;26:1572-1573.
- 12) Law CW, Chen Y, Shi W, Smyth GK. voom: Precision weights unlock linear model analysis tools for RNA-seq read counts. *Genome Biol* 2014;15:R29.
- 13) Therneau TM, Grambsch PM. *Modeling Survival Data: Extending the Cox Model*. New York, NY: Springer; 2000.
- 14) Liu X, Guo GL, Kong B, Hilburn DB, Hubchak SC, Park S, et al. Farnesoid X receptor signaling activates the hepatic X-box binding protein 1 pathway in vitro and in mice. *HEPATOLOGY* 2018;68:304-316.
- 15) Willy JA, Young SK, Stevens JL, Masuoka HC, Wek RC. CHOP links endoplasmic reticulum stress to NF-kappaB activation in the pathogenesis of nonalcoholic steatohepatitis. *Mol Biol Cell* 2015;26:2190-2204.
- 16) Vesterhus M, Holm A, Hov JR, Nygard S, Schruppf E, Melum E, et al. Novel serum and bile protein markers predict primary sclerosing cholangitis disease severity and prognosis. *J Hepatol* 2017;66:1214-1222.
- 17) Zweers SJ, Shiryayev A, Komuta M, Vesterhus M, Hov JR, Perugorria MJ, et al. Elevated interleukin-8 in bile of patients with primary sclerosing cholangitis. *Liver Int* 2016;36:1370-1377.
- 18) Trauner MH, Gindin Y, Zhou JZ, Huss R, Chung C, Subramanian M, et al. RNA-Seq from patients with primary sclerosing cholangitis identifies a fibrosis-independent gene expression signature that predicts clinical events. *HEPATOLOGY* 2019;70:758A-759A.
- 19) Yoshida H. ER stress and diseases. *FEBS J* 2007;274:630-658.
- 20) Dara L, Ji C, Kaplowitz N. The contribution of endoplasmic reticulum stress to liver diseases. *HEPATOLOGY* 2011;53:1752-1763.
- 21) Henkel AS, LeCuyer B, Olivares S, Green RM. Endoplasmic reticulum stress regulates hepatic bile acid metabolism in mice. *Cell Mol Gastroenterol Hepatol* 2017;3:261-271.
- 22) Bochkis IM, Rubins NE, White P, Furth EE, Friedman JR, Kaestner KH. Hepatocyte-specific ablation of Foxa2 alters bile acid homeostasis and results in endoplasmic reticulum stress. *Nat Med* 2008;14:828-836.
- 23) Liu X, Henkel AS, LeCuyer BE, Hubchak SC, Schipma MJ, Zhang E, et al. Hepatic deletion of X-box binding protein 1 impairs bile acid metabolism in mice. *J Lipid Res* 2017;58:504-511.
- 24) Ozcan U, Yilmaz E, Ozcan L, Furuhashi M, Vaillancourt E, Smith RO, et al. Chemical chaperones reduce ER stress and

restore glucose homeostasis in a mouse model of type 2 diabetes. *Science* 2006;313:1137-1140.

- 25) Lawless MW, Greene CM, Mulgrew A, Taggart CC, O'Neill SJ, McElvaney NG. Activation of endoplasmic reticulum-specific stress responses associated with the conformational disease Z alpha 1-antitrypsin deficiency. *J Immunol* 2004;172:5722-5726.
- 26) Trauner M, Gindin Y, Jiang Z, Chung C, Subramanian GM, Myers RP, et al. Methylation signatures in peripheral blood are associated with marked age acceleration and disease progression in patients with primary sclerosing cholangitis. *JHEP Rep* 2020;2:100060.
- 27) Horvath S. DNA methylation age of human tissues and cell types. *Genome Biol* 2013;14:R115.
- 28) Horvath S, Levine AJ. HIV-1 infection accelerates age according to the epigenetic clock. *J Infect Dis* 2015;212:1563-1573.
- 29) Loomba R, Gindin Y, Jiang Z, Lawitz E, Caldwell S, Djedjos CS, et al. DNA methylation signatures reflect aging in patients with nonalcoholic steatohepatitis. *JCI Insight* 2018;3:96685.
- 30) Brown MK, Naidoo N. The endoplasmic reticulum stress response in aging and age-related diseases. *Front Physiol* 2012;3:263.

Supporting Information

Additional Supporting Information may be found at onlinelibrary.wiley.com/doi/10.1002/hep.31488/suppinfo.